Image Reconstruction from TE Scattering Data Using Equation of Strong Permittivity Fluctuation

Jianglei Ma, *Member, IEEE*, Weng Cho Chew, *Fellow, IEEE*, Cai-Cheng Lu, *Senior Member, IEEE*, and Jiming Song, *Senior Member, IEEE*

***Abstract*—Compared to the TM case, the inverse scattering problem for the TE incident field is more complicated due to its stronger nonlinearity. This work provides an effective method for the reconstruction of two-dimensional (2-D) inhomogeneous dielectric objects from TE scattering data. The algorithm applies the distorted Born iterative method to the integral equation of strong permittivity fluctuation to reconstruct scatterers with high-permittivity contrast. Numerical simulations are performed and the results show that the distorted Born iterative method (DBIM) for strong permittivity fluctuation (SPF–DBIM) converges faster and can obtain better reconstructions for objects with larger dimensions and higher contrasts in comparison with ordinary DBIM. A frequency hopping technique is also applied to further increase the contrast.**

***Index Terms*—Electromagnetic scattering, inverse problems.**

I. Introduction

In microwave imaging, one tries to reconstruct the shape or the dielectric profile or both of an unknown object from the scattering microwave data measured outside. Until now, most two-dimensional (2-D) microwave inverse scattering algorithms developed were for TM wave illuminations in which the vectorial problem can be simplified to a scalar one [1]–[13], while much less work has been reported on the more complicated TE case [5], [14]–[16]. The combination of TE and TM polarizations should improve the quality of reconstruction. On the other hand, the inverse scattering algorithm for TE wave illuminations can also be used to solve the variable-density acoustic-wave scattering problems and can be easily extended to three-dimensional (3-D) cases.

In previous work on TE wave inverse scattering, Joachimowicz *et al.* [5] used an iterative algorithm based on the Newton–Kantorovich method to reconstruct complex permittivity profiles for 2-D TE polarizations where *a priori* information is needed. With prior knowledge of the conductor's shape, Chiu and Liu [14] proposed an algorithm based on the method of moments (MoM) for reconstructing a conductor cylinder coated with dielectric materials illuminated by TE waves. Otto and Chew [15] developed the local shape-function algorithm that was applied to image 2-D dielectric objects with TE incident fields. Wen *et al.* [16] also presented a method for reconstructing the complex permittivity of a bounded inhomogeneous object from measured scattered field data with TE wave excitations. However, the contrasts of reconstructed objects in [15] and [16] are relatively low.

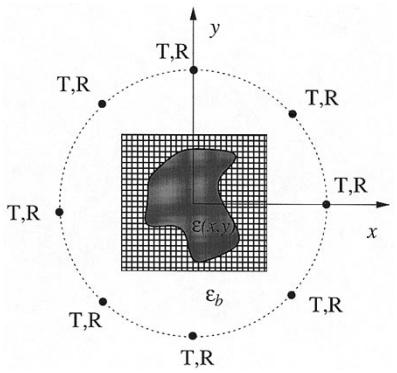

Fig. 1. Geometrical configuration of the problem. Transmitters "T" and receivers "R" are uniformly positioned on a circle that encloses the imaging region (which is denoted by the gridded square area). The actual object to be reconstructed is denoted as $\epsilon(x, y)$ (the shaded area) and the background permittivity is ϵ_b.

In this work, a new method is introduced to solve the inverse scattering problem for a TE wave impinging on 2-D dielectric objects with high contrasts without any *a priori* knowledge of the contrast and the size of the object. This inversion algorithm is based on the equation of strong permittivity fluctuation and the distorted Born iterative method (DBIM) [3]. In Section II we first present the formulation of the method and then give the numerical simulations in Section III. The numerical results show that in the forward problem, the new forward solver converges faster; and in the inverse problem, the new inverse solver can reconstruct higher contrast profiles with better quality compared to plain DBIM. Finally, some conclusions are drawn in Section IV. A time factor of $\exp(-i\omega t)$ is implied in this paper and suppressed.

II. Formulation

The geometry considered is shown in Fig. 1. The cylindrical dielectric object with an arbitrary cross section is inhomogeneous in the xy plane, but it is invariant in the z direction and is surrounded by a background medium of permittivity ϵ_b. In the case of multiple views, the object is illuminated successively by magnetic line sources (TE polarization) indicated as T in Fig. 1 with N_t different angles of incidence. The receivers indicated as R are also located on a circle around the object and can

Manuscript received July 31, 1997; revised October 21, 1999. This work was supported by the Office of Naval Research under Grant N00014-95-1-0872, the National Science Foundation under Grant NSF ECS 93-02145 and Air Force Office of Scientific Research (AFOSR) under a MURI grant.

The authors are with the Department of Electrical and Computer Engineering, University of Illinois at Urbana-Champaign, Urbana, IL 61801-2991 USA (email: w-chew@uiuc.edu).

Publisher Item Identifier S 0018-926X(00)01654-9.

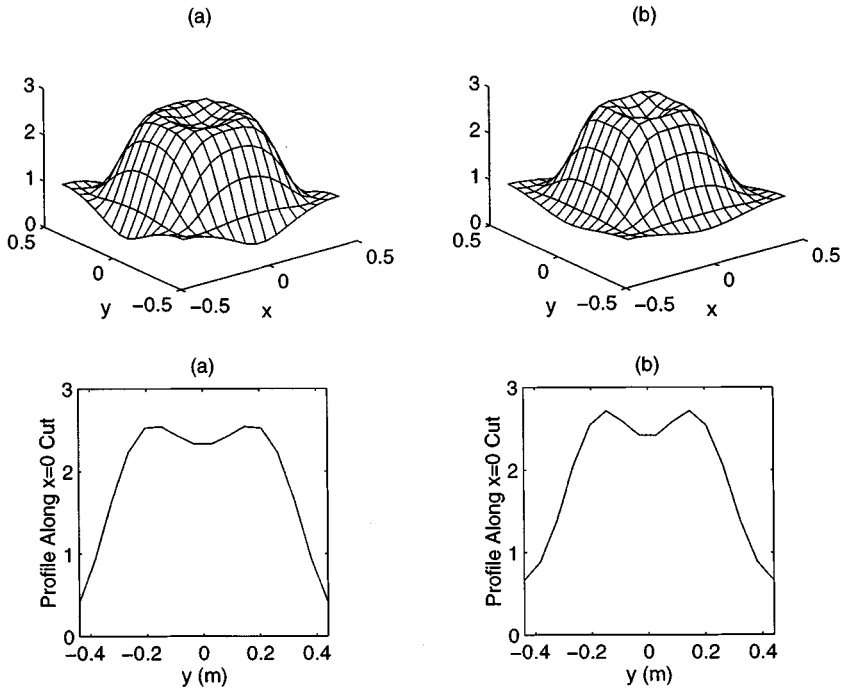

Fig. 2. Comparison of images reconstructed using (a) DBIM and (b) SPF-DBIM for $\epsilon_r = 3$ after eight iterations. (The dimensions of the object are $0.44\lambda_0 \times 0.44\lambda_0$. The reconstruction region consists of 16×16 cells, whose cell size is $0.055\lambda_0 \times 0.055\lambda_0$.)

measure the scattered electric field at several discrete angles ϕ_i, $i = 1, 2, \cdots, N_r$.

The total electric field $\boldsymbol{E}(\boldsymbol{r})$ satisfies the following vectorial wave equation:

$$\nabla \times \nabla \times \boldsymbol{E}(\boldsymbol{r}) - k^2 \boldsymbol{E}(\boldsymbol{r}) = iw\mu \boldsymbol{J}(\boldsymbol{r}) \tag{1}$$

where $\boldsymbol{J}(\boldsymbol{r})$ is the current density of the radiating source, $k^2 = \omega^2 \epsilon(\boldsymbol{r})\mu$, and $\epsilon(\boldsymbol{r})$ is the permittivity profile to be reconstructed. An integral equation can be derived for the total electric field [1] (the scalar form integral equation for the z-component of magnetic field may also be used for TE wave inversion problem. However, it turns out that the vector form integral equation has a better performance than the scalar one. This has been demonstrated by Kooij and van den Berg [17])

$$\boldsymbol{E}(\boldsymbol{r}) = \boldsymbol{E}^i(\boldsymbol{r}) + \int d\boldsymbol{r}' \overline{\boldsymbol{G}}(\boldsymbol{r}, \boldsymbol{r}') \Delta k^2 \cdot \boldsymbol{E}(\boldsymbol{r}') \tag{2}$$

where

$$\overline{\boldsymbol{G}}(\boldsymbol{r}, \boldsymbol{r}') = \left(\overline{\boldsymbol{I}} - \frac{1}{k_b^2} \nabla \nabla' \right) g(\boldsymbol{r}, \boldsymbol{r}') \tag{3}$$

is the dyadic Green's function for homogeneous background medium ϵ_b, $\overline{\boldsymbol{I}}$ is the 2-D identity operator, $g(\boldsymbol{r}, \boldsymbol{r}')$ is the 2-D scalar Green's function $k_b^2 = \omega^2 \mu \epsilon_b$ and $\Delta k^2 = k^2 - k_b^2$.

Because $\overline{\boldsymbol{G}}(\boldsymbol{r}, \boldsymbol{r}')$ has a singularity of the order of $|\boldsymbol{r} - \boldsymbol{r}'|^{-2}$, the integral equation (2) is indeterminate if the field point is inside the source region. In order to overcome this difficulty, we exclude a small volume V_s surrounding the field point at first and then let the small volume approach zero [1]. After extracting the singular part, (2) can be rewritten as

$$\left(\overline{\boldsymbol{I}} + \frac{\Delta k^2}{k_b^2} \overline{\boldsymbol{L}} \right) \cdot \boldsymbol{E}(\boldsymbol{r}) = \boldsymbol{E}^i(\boldsymbol{r}) + P.V. \int d\boldsymbol{r}' \overline{\boldsymbol{G}}(\boldsymbol{r}, \boldsymbol{r}') \Delta k^2 \cdot \boldsymbol{E}(\boldsymbol{r}') \tag{4}$$

where $P.V. \int$ stands for a shape dependent principal value integral, $\overline{\boldsymbol{L}}$ is a dyad dependent on the shape of V_s. Defining $\boldsymbol{F}(\boldsymbol{r}) = (\overline{\boldsymbol{I}} + (\Delta k^2)/(k_b^2)\overline{\boldsymbol{L}}, \cdot \boldsymbol{E}(\boldsymbol{r})$ and $\overline{\boldsymbol{\xi}} = \Delta k^2 (\overline{\boldsymbol{I}} + (\Delta k^2)/(k_b^2)\overline{\boldsymbol{L}})^{-1}$, (4) becomes

$$\boldsymbol{F}(\boldsymbol{r}) = \boldsymbol{E}^i(\boldsymbol{r}) + P.V. \int d\boldsymbol{r}' \overline{\boldsymbol{G}}(\boldsymbol{r}, \boldsymbol{r}') \cdot \overline{\boldsymbol{\xi}} \cdot \boldsymbol{F}(\boldsymbol{r}') \tag{5}$$

which is the integral equation for strong permittivity fluctuation [18], [19].

We use the distorted Born iterative method (DBIM) described in [3] to reconstruct the permittivity profile of a scatterer based on measurement data $\boldsymbol{E}^{\text{sca}}_{\text{meas}}(r_R, r_T)$, where r_R and r_T are the locations of transmitters and receivers, respectively. To reconstruct the unknown permittivity profile by the Born iterative method, both the forward scattering problem and the inverse scattering problem are solved. In DBIM, the Green's function [appeared as the integration kernel in (5)] is also updated for each iteration.

To solve the forward scattering problem, we apply the method of moments (MoM) to transform (5) into a matrix equation. To this end, the solution region or the region of unknown field is discretized into N equal-sized subregions or cells. The cells are denoted by S_n, $n = 1, 2, \cdots, N$. Let $\boldsymbol{r}_n$ be the center of cell

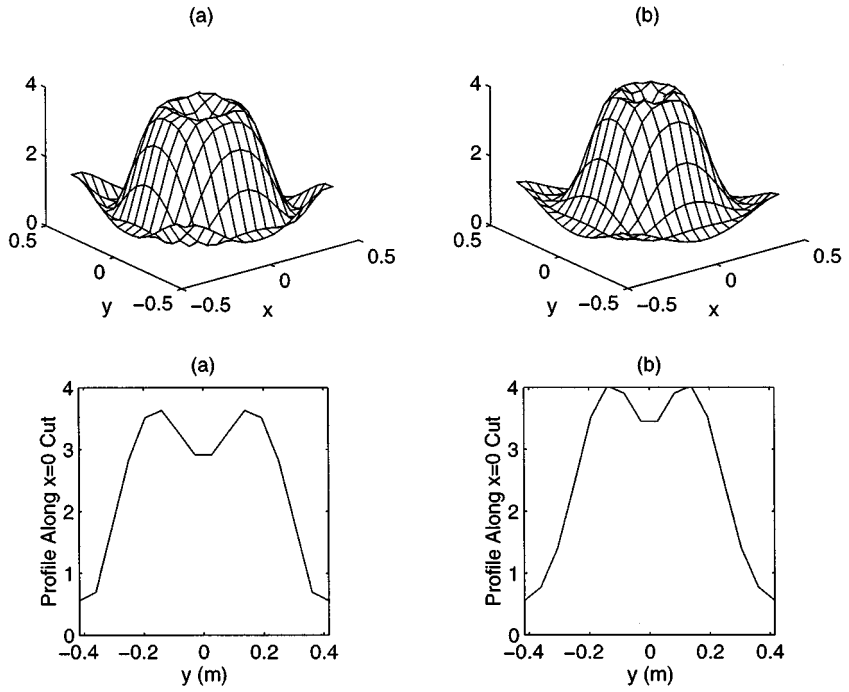

Fig. 3. Comparison of images reconstructed using (a) DBIM and (b) SPF-DBIM for $\epsilon_r = 4$ after 14 iterations. ($r = 0.5288$.The dimensions of the object are $0.44\lambda_0 \times 0.44\lambda_0$. The reconstruction region consists of 16×16 cells, whose cell size is $0.052\lambda_0 \times 0.052\lambda_0$.)

S_n and $\boldsymbol{F}_n = \boldsymbol{F}(\boldsymbol{r}_n)$, then $\boldsymbol{F}(\boldsymbol{r})$ can be approximated by the superposition of N pulse functions, i.e,

$$\boldsymbol{F}(\boldsymbol{r}) = \sum_{n=1}^{N} \boldsymbol{F}_n P(\boldsymbol{r} - \boldsymbol{r}_n) \tag{6}$$

where $P(\boldsymbol{r})$ is a pulse basis of unit amplitude

$$P(\boldsymbol{r}) = \begin{cases} 1, & \left\{|x| < \dfrac{\Delta x}{2}\right\} \times \left\{|y| < \dfrac{\Delta y}{2}\right\} \\ 0, & \text{otherwise} \end{cases} \tag{7}$$

and $\Delta x \Delta y$ is the cell size.

Using (7) in (5) and testing the resultant equation by impulse functions $\delta(\boldsymbol{r} - \boldsymbol{r}_m)$, $m = 1, 2, \cdots, N$, we obtain a set of N linear algebraic equations for $\boldsymbol{F}_n$, $n = 1, 2, \cdots, N$

$$\boldsymbol{F}_m = \boldsymbol{E}^i(\boldsymbol{r}_m) + \sum_{n=1}^{N} \overline{\boldsymbol{G}}_{mn} \cdot \overline{\boldsymbol{\xi}}_n \cdot \boldsymbol{F}_n, \qquad m = 1, 2 \cdots, N \tag{8}$$

in which

$$\overline{\boldsymbol{G}}_{mn} = P.V. \int d\boldsymbol{r}' \overline{\boldsymbol{G}}(\boldsymbol{r}_m, \boldsymbol{r}') P(\boldsymbol{r}' - \boldsymbol{r}_n). \tag{9}$$

According to [20], the 2-D source dyad $\overline{\boldsymbol{L}}$ can be expressed as $\overline{\boldsymbol{I}}/2 = (\hat{x}\hat{x} + \hat{y}\hat{y})/2$ if the exclusion region is chosen as a circle. In this case, the dyad $\overline{\boldsymbol{\xi}}_n$ and the vector $\boldsymbol{F}_n$ in (8) become

$$\boldsymbol{F}_n = \left(1 + \frac{\Delta k_n^2}{2k_b^2}\right) \boldsymbol{E}_n, \qquad \overline{\boldsymbol{\xi}} = \Delta k_n^2 \left(1 + \frac{\Delta k_n^2}{2k_b^2}\right)^{-1} \overline{\boldsymbol{I}}.$$

A. Direct Scattering Solution

Each iteration in distorted Born iterative method (DBIM) must solve both the forward scattering problems for the unknown total field inside the object and the Green's function for inhomogeneous media. Therefore, an efficient forward solver plays an important role in the inverse scattering algorithm. We use the conjugate gradient-fast Fourier transform (CGFFT) to solve the forward scattering problem, which has been proven to be an efficient method [21]–[23].

The corresponding matrix expression for (8) is

$$(\overline{\boldsymbol{I}} - \overline{\boldsymbol{G}} \cdot \overline{\boldsymbol{\xi}}) \cdot \boldsymbol{F} = \boldsymbol{E}^i \tag{10}$$

where

$$\boldsymbol{E}^i = \begin{bmatrix} E_x^i \\ E_y^i \end{bmatrix}, \quad \boldsymbol{F} = \begin{bmatrix} F_x \\ F_y \end{bmatrix}$$
$$\overline{\boldsymbol{G}} = \begin{bmatrix} G_{xx} & G_{xy} \\ G_{yx} & G_{yy} \end{bmatrix}, \quad \overline{\boldsymbol{\xi}} = \begin{bmatrix} \xi & 0 \\ 0 & \xi \end{bmatrix}.$$

The term is a diagonal matrix with the diagonal terms

$$\frac{k^2 - k_b^2}{1 + \dfrac{k^2 - k_b^2}{2k_b^2}}.$$

The components E_α^i and $F_\alpha (\alpha = x, y)$ are $N \times 1$ matrices. The pth element in $\boldsymbol{E}_\alpha^i$ is the α-component of $\boldsymbol{E}^i(\boldsymbol{r}_p)$.

We apply the conjugate gradient (CG) algorithm to solve (10) iteratively. In each iteration, we use FFT to perform the matrix-vector multiply, which reduces the number of operations from $O(N^2)$ to $O(N \log_2 N)$.

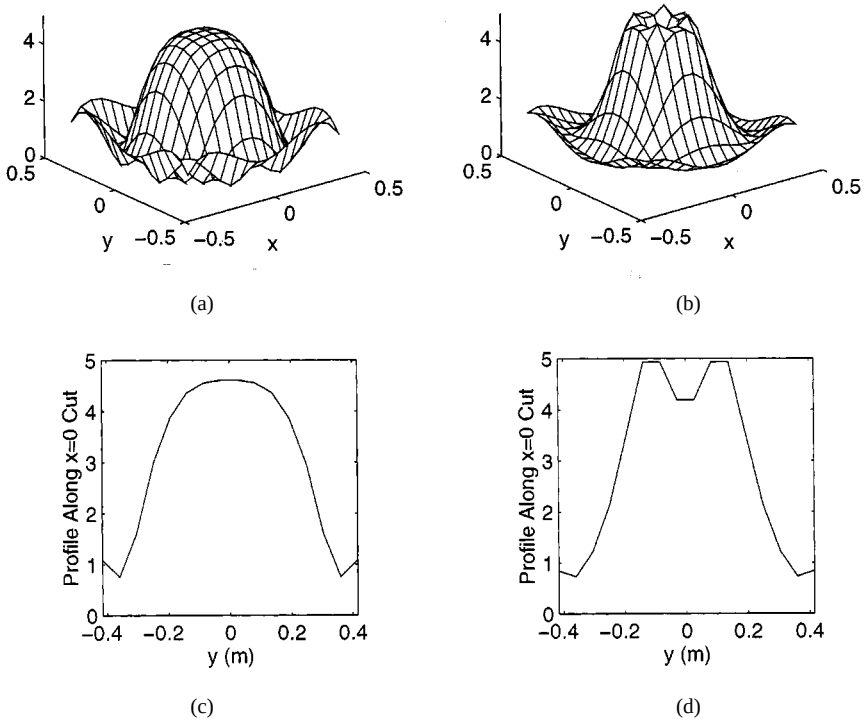

Fig. 4. Same comparison as in Fig. 3, with $\epsilon_r = 5$ after eight iterations.

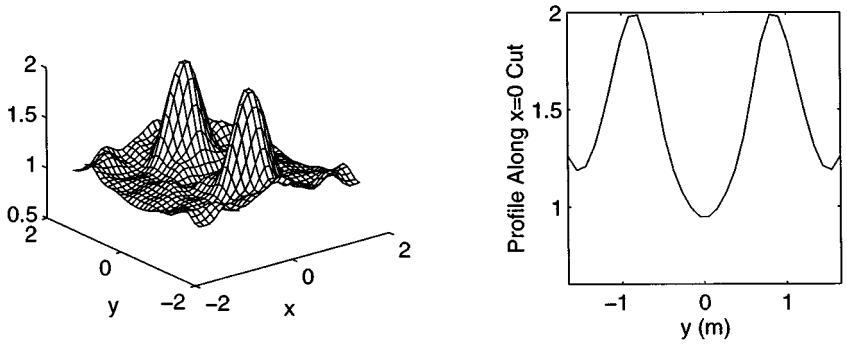

Fig. 5. Reconstruction by SPF-DBIM for $\epsilon_r = 2$. The objects are square cylinders with side length $\frac{3}{4}\lambda_0$. The reconstruction region consists of 32×32 cells and each cell is a small square of size $0.1034\lambda_0 \times 0.1034\lambda_0$.

B. Inverse Scattering Solution

In an inverse scattering problem, the permittivity profile of the object is reconstructed from measured scattering data. Because of multiple scattering, the measured data are nonlinearly related to the object function $\Delta\epsilon(\boldsymbol{r}') = \epsilon(\boldsymbol{r}') - \epsilon_b(\boldsymbol{r}')$, where $\epsilon(\boldsymbol{r}')$ is the unknown permittivity profile to be solved for and $\epsilon_b(\boldsymbol{r}')$ is a guessed or estimated permittivity profile that is assumed known. In the DBIM approach, an iterative procedure is used to optimize a cost function, which is a measure of the difference between the measured data and the simulation data calculated from an estimated object profile.

The cost function can be defined as a function of $\xi_1 = (\xi/k_0^2)$ as

$$\begin{aligned} S(\xi) &= \tfrac{1}{2}(\|\boldsymbol{E}^{\mathrm{sca}}(\xi_1) - \boldsymbol{E}^{\mathrm{sca}}_{\mathrm{meas}}\|^2 + \gamma\|\delta\xi_1\|^2) \\ &= \tfrac{1}{2}(\|E^{\mathrm{sca}}_x(\xi_1) - E^{\mathrm{sca}}_{x\mathrm{meas}}\|^2 + \|E^{\mathrm{sca}}_y(\xi_1) - E^{\mathrm{sca}}_{y\mathrm{meas}}\|^2 \\ &\quad + \gamma\|\delta\xi_1\|^2) \end{aligned} \tag{11}$$

where $\delta\xi = \xi_1^n - \xi_1^{n-1}$; ξ_1^n and ξ_1^{n-1} are the values of ξ_1 obtained in nth and $(n-1)$th iteration, respectively; γ is the regularization parameter; and the L_2 norm is assumed. As the inverse scattering problem is ill conditioned in nature, a regularization term $\gamma\|\delta\xi_1\|^2$ is introduced in the error function in (11). It should be pointed out that this is not the only way to circumvent the inherently ill-conditioned nature of the inverse scattering problems.

The conjugate gradient algorithm, a Newton-type minimization method, is used to minimize the cost function [21]. In each iteration, we need to calculate the gradient of the functional and the Hessian, where the gradient is required to calculate the conjugate vector and the Hessian to find the step size. In this algorithm, it is assumed that the functional changes quadratically with respect to the object profile by a linearization approximation.

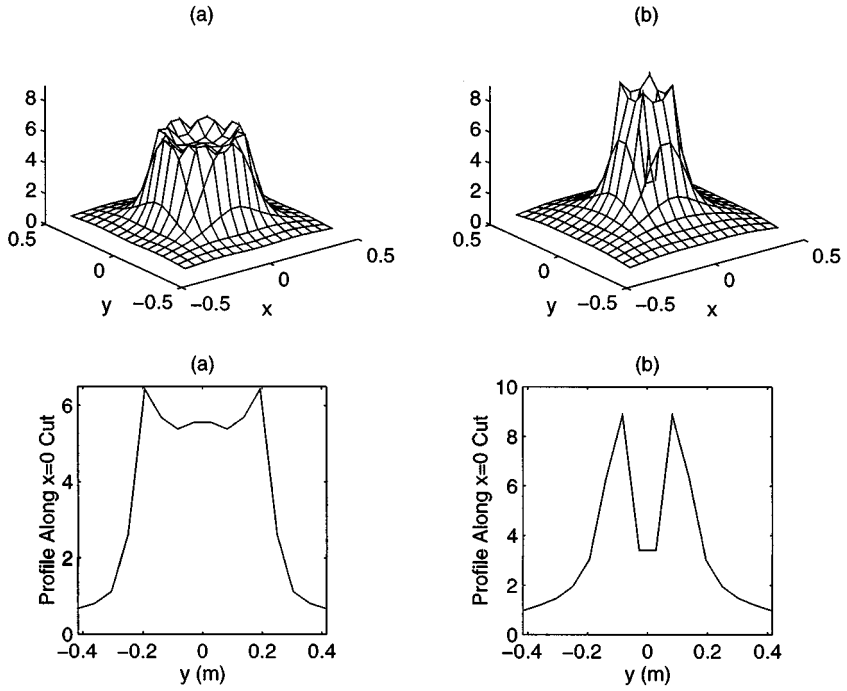

Fig. 6. The reconstruction of a square cylinder with $\epsilon_r = 6$ using the frequency-hopping approach from (a) data at three frequencies (100, 200, and 300 MHz) are used and (b) data at two frequencies (100 and 300 MHz) are used. The result in (a) is better than that in (b).

The linear relationship between δE_{x_p} and $\delta\xi_1$ can be written as

$$\delta E_{x_p} = \mathcal{F}_{x_p}\delta\xi_1 \tag{12}$$

where $\mathcal{F}_{x_p} = \delta E^{\text{sca}}_{x_p}/\delta\xi_1$ is Fréchet derivative operator and $\delta E_{x_p} = E^{\text{sca}}_{x_p} - E^{\text{sca}}_{x_p\text{meas}}(p = 1, 2; x_1 = x, x_2 = y)$. When $\mathcal{F}_{x_p}$, is determined, the gradient and the Hessian can be calculated.

The scattered field $E^{\text{sca}}_{x_p}$ can be expressed as

$$E^{\text{sca}}_{x_p} = \sum_{q=1}^{2} G'_{x_p x_q}\xi F_{x_q} \tag{13}$$

where

$$\overline{\boldsymbol{G}}' = \begin{bmatrix} G'_{xx} & G'_{xy} \\ G'_{yx} & G'_{yy} \end{bmatrix}$$

is the Green's function for the homogeneous background medium with the receiver locations as the field points $F_{x_q} = (1 + (\Delta k_n^2))/(2k_b^2)E_{x_q}$, and $E_{x_q}(q = 1, 2)$ is the x or y component of the total field at each grid point.

Using (13) and (12), we can show that

$$\mathcal{F}_{x_p} = k_0^2 \sum_{q=1}^{2} \left(1 + \frac{\Delta k_n^2}{2k_b^2}\right) \tilde{G}'_{x_p x_q}\mathcal{D}(E_{x_q}) \tag{14}$$

where $\mathcal{D}$ is an operator that converts a vector into a square diagonal matrix, $\tilde{G}'_{x_p x_q}$ is the Green's function for the inhomogeneous background medium, and the field points are at the receiver locations.

To calculate the Fréchet derivative operator, the reconstructed value of $\epsilon(\boldsymbol{r}')$ is used as the new $\epsilon_b(\boldsymbol{r}')$ after each iteration step of minimizing the cost function. Therefore, the Green's function $\tilde{G}'(\boldsymbol{r}, \boldsymbol{r}')$ has to be updated in each iteration. To calculate the Green's function numerically, the matrix solution needed is exactly that used for solving the forward scattering problem [which is given by (8)] [3]. In other words, the same process for solving the forward scattering problem is applied to obtain the numerical Green's function for the updated permittivity profile (this profile is considered as the background of the next Born iteration).

III. Numerical Results

Using the algorithm described above, we have developed a program to solve both the forward scattering problems and inverse scattering problems. The forward scattering solution is validated with the Mie series solution for a number of uniform circular dielectric cylinders. In the following, we present some numerical reconstruction examples. It should be mentioned that the forward solver (SPF–CGFFT) is not used to generate the synthetic measured data needed for reconstruction. Instead, the "measured data" was generated by a different code. The latter solves (2) directly with different singularity handling process and only the region with $\epsilon(\boldsymbol{r}) - \epsilon_b \neq 0$ is considered as the solution domain (this is in contrast to the CGFFT algorithm in which the solution domain is a square area that consists of the true object as well as a portion of background). This arrangement is intended to avoid the so called "inverse crime" as the two forward scattering codes do not generate numerically identical scattered fields for identical configurations.

In our numerical simulations, 16 transmitters and 16 receivers are equally placed on a circle of radius 10.0 m. The operating frequency is 300 MHz. The objects are 2-D dielectric cylinders.

At first, we compare the images reconstructed by DBIM and SPF–DBIM. Figs. 2, 3, and 4 are the comparisons of the images reconstructed by DBIM and SPF–DBIM. The objects are square cylinders of side length $0.44\lambda_0$ and with the contrast of

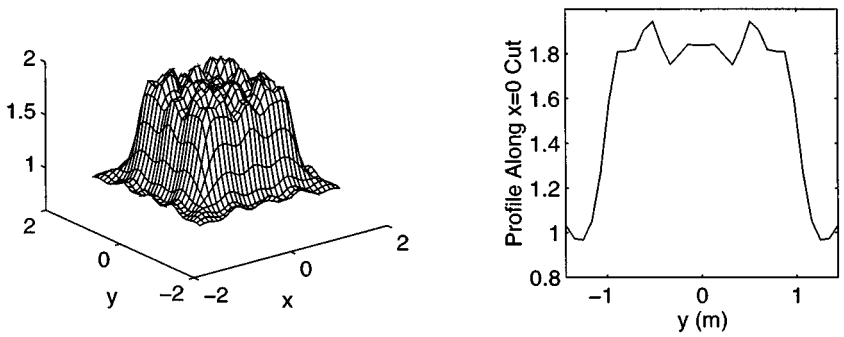

Fig. 7. Reconstruction of a square cylinder with dimensions and contrast of $2\lambda_0 \times 2\lambda_0$ and 1.8, respectively.

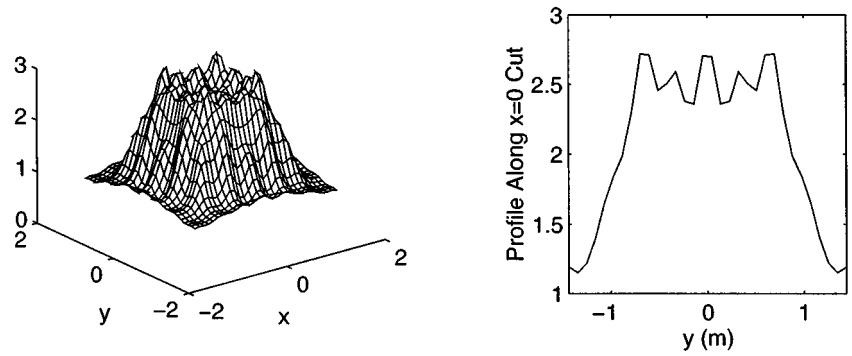

Fig. 8. Reconstruction of a square cylinder with dimensions and contrast of $2\lambda_0 \times 2\lambda_0$ and 2.5, respectively.

$3:1$, $4:1$, and $5:1$, respectively. The reconstruction region consists of 16×16 square cells. The size of each cell is $0.055\lambda_0 \times 0.055\lambda_0$ in Fig. 2, and $0.052\lambda_0 \times 0.052\lambda_0$ in Figs. 3 and 4. In each example, the number of iterations for both methods are the same. These examples indicate that both the shapes and the permittivity values obtained from SPF–DBIM are closer to the real objects than are those obtained from DBIM. Also the background noise of SPF–DBIM is much lower than that of DBIM. The difference between two methods becomes more obvious when the permittivity of the reconstructed object increases. SPF–DBIM is, therefore, superior to DBIM, especially in the reconstruction of a high-contrast object. In [15], the contrast of $2:1$ marks the maximum region of convergence for DBIM with TE wave illuminations. In our simulations here, however, we found that when the contrast is beyond $2:1$, DBIM still converges. The reason is that in [15], the object is reconstructed from the H_z, scattering field, whereas in this paper, the scattering field includes E_x and E_y components, which provide more information about the object to be reconstructed.

In the next example, we use SPF–DBIM to reconstruct two distinct square cylinders of diameter $(3/4)\lambda_0$ with $\epsilon_r = 2$. The distance between the two cylinders is also $(3/4)\lambda_0$. The reconstruction region was subdivided into 32×32 subsquares of size $0.1034\lambda_0 \times 0.1034\lambda_0$. Fig. 5 gives the reconstructed permittivity distributions.

When the reconstructed object becomes large compared to the wavelength or when the contrast of the inhomogeneity becomes large, the nonlinear effect becomes more pronounced. To reconstruct the object with larger dimensions and higher contrasts without *a priori* information, we applied the frequency-hopping technique described in [22] in some cases. In the frequency hopping approach, the permittivity profile reconstructed from lower frequency data is used as the initial guess to the higher frequency problem. After several steps of frequency hopping, we can acquire a much better image than that obtained by using the high-frequency data directly. The reason is that at lower frequencies, the Born-type approximation is a better approximation. Therefore, the low-frequency data help to alleviate the nonlinear effect of the problem by providing initial guesses to the higher frequency data.

In Fig. 6, the reconstruction is given for a square cylinder of diameter $0.44\lambda_0$ with $\epsilon_r = 6$. Three frequency-hopping steps are used in this reconstruction. For comparison, the reconstruction by two frequency-hopping steps is also given. The image quality from the three frequency-hopping steps is better than that of the two frequency-hopping steps.

In the following examples, we increase the dimensions of the object. In Figs. 7 and 8, the dimensions of the objects are $2\lambda_0 \times 2\lambda_0$, and the contrasts are 1.8 and 2.5, respectively. The whole reconstructed region consists of 32×32 cells and the size of each cell is $0.09\lambda_0 \times 0.09\lambda_0$.

IV. Conclusion

The introduction of the strong permittivity fluctuation theory in the DBIM gives an efficient electromagnetic inverse scat-

tering algorithm for 2-D TE polarization case. The comparison has been made between the method developed in this work and the ordinary DBIM. The results show that the new method is superior because of its faster convergence speed and better image quality. By using multifrequency information, we have reconstructed the objects with larger dimensions and higher contrasts than was previously possible. No *a priori* information is needed in this inverse scattering algorithm.

REFERENCES

[1] W. C. Chew, *Waves and Fields in Inhomogeneous Media*. New York: Van Nostrand Reinhold, 1990.

[2] Y. M. Wang and W. C. Chew, "An iterative solution of two-dimensional electromagnetic inverse scattering problem," *Int. J. Imag. Syst. Tech.*, vol. 1, pp. 100–108, 1989.

[3] W. C. Chew and Y. M. Wang, "Reconstruction of two-dimensional permittivity distribution using the distorted Born iterative method," *IEEE Trans. Med. Imag.*, vol. 9, pp. 218–225, June 1990.

[4] J. C. Bolomey and C. Pichot, "Microwave tomography: From theory to practical imaging systems," *Int. J. Imag. Syst. Tech.*, vol. 2, pp. 144–156, 1990.

[5] N. Joachimowic, C. Pichot, and J.-P. Hugonin, "Inverse scattering: An iterative numerical method for electromagnetic imaging," *IEEE Trans. Antennas Propagat.*, vol. 39, pp. 1742–1752, Sept. 1991.

[6] M. Moghaddam and W. C. Chew, "Nonlinear two-dimensional velocity profile inversion using time domain data," *IEEE Trans. Geosci. Remote Sensing*, vol. 30, pp. 147–156, Jan. 1992.

[7] W. C. Chew and G. P. Otto, "Microwave imaging of multiple conducting cylinders using local shape functions," *IEEE Microwave Guided Wave Lett.*, vol. 2, pp. 284–286, July 1992.

[8] G. P. Otto and W. C. Chew, "Microwave inverse scattering-local shape function imaging for improved resolution of strong scatterers," *IEEE Trans. Microwave Theory Tech.*, vol. 42, pp. 137–141, Jan. 1994.

[9] A. Roger, "Newton–Kantorovich algorithm applied to an electromagnetic inverse problem," *IEEE Trans. Antennas Propagat.*, vol. AP-29, pp. 232–238, Mar. 1981.

[10] D. Colton and P. Monk, "A novel method for solving the inverse scattering problem for time-harmonic acoustic waves in the resonance region II," *SIAM J. Appl. Math.*, vol. 46, pp. 506–523, 1986.

[11] C. C. Chiu and Y.-W. Kiang, "Inverse scattering of a buried conducting cylinder," *Inverse Problem*, vol. 7, pp. 187–202, 1991.

[12] R. E. Kleinman and P. M. Van Den Berg, "Nonlinearized approach to profile inversion," *Int. J. Imag. Syst. Tech.*, vol. 2, pp. 119–126, 1990.

[13] K. Belkebir, R. E. Kleinman, and Christian Pichot, "Microwave imaging-location and shape reconstruction from multifrequency scattering data," *IEEE Trans. Microwave Theory Tech.*, vol. 45, pp. 469–476, Apr. 1997.

[14] C. C. Chiu and P. T. Liu, "Image reconstruction of a complex cylinder illuminated by TE waves," *IEEE Trans. Microwave Theory Tech.*, vol. 44, pp. 1921–1952, Oct. 1996.

[15] G. P. Otto and W. C. Chew, "Inverse scattering of H_z waves using local shape-function imaging: A T-matrix formulation," *Int. J. Imag. Syst. Tech.*, vol. 5, pp. 22–27, 1994.

[16] L. Wen, R. E. Kleinman, and P. M. Van Den Berg, "Two-dimensional profile inversion—The TE case," in *Proc. 1995 URSI Int. Symp. Electromagn. Theory*, St. Petersburg, Russia, July 1995, pp. 160–162.

[17] B. J. Kooij and P. M. van den Berg, "Nonlinear inversion in TE scattering," *IEEE Trans. Microwave Theory Tech.*, vol. 46, pp. 1704–17l2, Nov. 1998.

[18] L. Tsang, J. A. Kong, and R. T. Shin, *Theory of Microwave Remote Sensing*. New York: Wiley, 1985.

[19] V. V. Tamoikin, "The average field in a medium having strong anisotropic inhomogeneities," *Radiophys. Quantum Electron.*, vol. 14, pp. 228–233, 1971.

[20] A. D. Yaghjian, "Electric dyadic Green's functions in the source region," *Proc. IEEE*, vol. 68, pp. 248–263, Feb. 1980.

[21] J. H. Richmond, "Scattering by a dielectric cylinder of arbitrary cross section shape," *IEEE Trans. Antennas Propagat.*, vol. AP-13, pp. 334–341, May 1965.

[22] J. H. Lin, "A study of iterative method on forward and inverse scattering problems," Ph.D. dissertation, Univ. Illinois at Urbana-Champaign, 1995.

[23] W. C. Chew and J. H. Lin, "A frequency-hopping approach for microwave imaging of large inhomogeneous bodies," *IEEE Microwave Guided Lett.*, vol. 5, pp. 439–441, Dec. 1995.

[24] P. Zwamborn and P. M. van den Berg, "A weak form of the conjugate fradient FFT method for two-dimensional TE scattering problems," *IEEE Trans. Microwave Theory Tech.*, vol. 39, pp. 953–960, Apr. 1995.

Jianglei Ma (S'92–M'93) received the B.E., M.E., and Ph.D. degrees in electrical engineering from Southeast University, Nanjing, China, in 1982, 1985, and 1992, respectively.

In 1985, she joined the Electronic Engineering Department, Southeast University, where she was involved in the teaching and the research on lasers, electromagnetics, and millimeter-wave techniques as an Assistant, Lecturer, Associate Professor, and Professor. From 1996 to 1997 she was with the Electrical and Computer Engineering Department, Center for Computational Electromagnetics, UIUC, as a Visiting Associate Professor, where she was involved in the research on inverse scattering and image reconstruction. She is currently with Wavesat Telecom, Inc. Her interests are in wirelss telecommunications system, broad-band modem design, and fast DSP algorithm development.

Weng Cho Chew (S'79–M'80–SM'86–F'93) was born on June 9, 1953, in Maylasia. He received the B.S. degree in 1976, the M.S. and Engineer's degrees, in 1978, and the Ph.D. degree, in 1980, all in electrical engineering from the Massachusetts Institute of Technology, Cambridge.

From 1981 ato 1985, he was with Schlumberger-Doll Research, Ridgefield, CT. While there, he was a Program Leader and later a Department Manager. From 1985 to 1990 he was an Associate Professor with the Unversity of Illinois, Urbana-Champaign. He is currently a Professor there, teaching graduate courses in waves and fields in inhomogeneous media and theory of microwave and optical waveguides, as well as supervising a graduate research program. He has been an associate editor of the *Journal of Electromagnetic Waves and Applications* (1996–present) and *Microwave Optical Technology Letters* (1996–present). He was also and associate editor with the *International Journal of Imaging Systems and Technology* (1989–1994), and has been a guest editor for *Radio Science* (1986), *International Journal of Imaging Systems and Technology* (1989), and *Electromagnetics* (1995). From 1989 to 1993 he was the Associate Director of the Advanced Construction Technology Center, University of Illinois, Urbana-Champaign. He has authored *Waves and Fields in Inhomogeneous Media* and has published over 200 scientific journal articles and presented over 270 conference papers. His recent research interest has been in the area of wave propagation, scattering, inverse scattering, and fast algorithms related to scattering, inhomogeneous media for geophysical subsurface sensing and nondestructive testing applications. Previously, he also analyzed electrochemical effects and dielectric properties of composite materials, microwave and optical waveguides, and microstrip antennas.

Dr. Chew was an NSF Presidential Young Investigator in 1986. He has recently been selected to receive the year 2000 IEEE Graduate Teaching Award. He was recently named Founder Professor of Engineering of the University of Illinois. He was also an AdCom member of the IEEE Geoscience and Remote Sensing Society. Since 1984 he has been an associate editor of the IEEE TRANSACTIONS ON GEOSCIENCE AND REMOTE SENSING. He is a member of Eta Kappa Nu, Tau Beta Pi, URSI Commissions B and F, and an active member of the Society of Exploration Geophysics.

Cai-Cheng Lu (S'93–M'95–SM'99) received the B.S. and M.S. degrees from Beijing University of Aeronautics and Astronautics, China, in 1983 and 1986, respectively, and the Ph.D. degree from University of Illinois at Urbana-Champaign, in 1995.

From 1986 to 1991, he was with the Department of Electronic Engineering, University of Aeronautics and Astronautics, China. From 1992 to 1997 he was in the Department of Electrical and Computer Engineering, University of Illinois at Urbana-Champaign, first as a Graduate Research Assistant and later as a Research Scientist. He has been working on antenna design and measurement, fast algorithms for electromagnetic scattering, and inverse scattering. He participated in the development of the fast Illinois solver code (FISC). In 1998 he joined Demaco, Inc., where he worked on asymptotic techniques for radar scattering predicitons. predictions. Currently, he is an Assistant Professor at the Universtiy of Kentucky, Lexington. His research interests include fast algorithms for wave scattering and inverse scattering, antenna analysis and design, and electromagnetic biomedical applications.

Dr. Lu is the recipient of the 2000 Young Investigator Award from the Office of Naval Research. He is a member of Phi Kappa Phi.

Jiming Song (S'92–M'95–SM'99) received the B.S. and M.S. degrees, both in physics, from Nanjing Universtiy, China, in 1983 and 1988, respectively, and the Ph.D. degree in electrical engineering from Michigan State University, East Lansing, in 1993.

From 1983 to 1985, he worked in the Department of Microwave Engineering of Beijing Broadcasting College, China. From 1993 he worked as a Postdoctoral Research Associate at the University of Illinois at Urbana-Champaign. He is currently a Research Scientist and Visiting Assistant Professor at the University of Illinois at Urbana-Champaign and a Research Scientist at SAIC-DEMACO. He is the principal author of the FAST Illinois Solver Code. His research has dealt with the wave scattering using fast algorithms, the wave interaction with inhomogeneous media, transient electromagnetic field, and high Tc superconductive electronics.

Dr. Song is a member of Phi Kappa Phi and, in 1992, was the recipient of the Outstanding Academic Award from the College of Engineering, Michigan State University.